Electrical and Electrochemical Performance Characteristics of Small Commercial Li-ion Cells

G. Nagasubramanian, E. P. Roth, and D. Ingersoll
1521 Lithium Battery R & D, Sandia National Laboratories, Albuquerque, NM 87185

Abstract

Advanced rechargeable lithium-ion batteries are presently being developed and commercialized worldwide for use in consumer electronics, military and space applications. At Sandia National Laboratories we have used different electrochemical techniques such as impedance and charge/discharge at ambient and subambient temperatures to probe the various electrochemical processes that are occurring in Li-ion cell. The purpose of this study is to identify the component that reduces the cell performance at subambient temperatures. Our impedance data suggest that while the variation in the electrolyte resistance between room temperature and -20°C is negligible the anode electrolyte interfacial resistance increases by an order of magnitude in the same temperature regime. We believe that the solid electrolyte interface (SEI) layer on the carbon anode may be responsible for the increase in cell impedance. We have also evaluated the cells in hybrid mode with capacitors. High-current operation in the hybrid mode allowed full usage of the Li-ion cell capacity at 25°C and showed a factor of 5 improvement in delivered capacity at -20°C.

Introduction

Because of a favorable combination of high-energy density and power density, Li-ion cells are being increasingly used, in recent years, in different applications[1]. However, the low temperature performance requirements, as well as the need for high capacity cells make these applications a great challenge to Li-ion cell developers. Pulsed-current applications of battery systems are becoming more demanding and more common. Communication systems using high-power bursts of digitized and compressed voice and data are of special interest to the military. These applications and other similar uses requiring intermittent high -power usage of present batteries can result in significant reduction of available battery capacity when fixed threshold voltage criteria are required for operation. Given the nature of the lithium-ion chemistry the low-temperature performance of the cells may not be very good. At Sandia National Laboratories we are currently evaluating Li-ion cells and Li-ion/capacitor hybrids to define the electrical performance envelope at different temperatures.

Little published data are available in the literature on the low-temperature electrical performance characteristics of the lithium-ion cells[2] and fewer published data are available for hybrid power sources[3,4]. This paper reports (1) our electrical and electrochemical test results at different temperatures on Li-ion cells, and (2) on a hybrid power system combining Li-ion cells and double-layer capacitors to extend the current capabilities of the battery system and allow full usage of the electrochemical capacity.

Experimental

Lithium-ion cells of three different sizes (18650, 17500 cylindrical and 48.3x25.4x7.6 mm prismatic) were evaluated. Before welding tabs to the cells for electrical connections, both their weights and physical dimensions were measured. Average values for weights and computed cell volumes are given in Table 1 along with the cell type, capacity, manufacturer, and the number of cells tested. Initially, the cells were charged and discharged at room temperature (for at least 5 cycles) at a very low rate (~C/20) as "break-in" cycles. The discharge capacities given in Table 1 represent the average of 5 cycles per cell and are also averaged over the number of cells tested for that type. The nominal (rated) cell capacity is slightly higher than the measured discharge capacity except for the Sony and Sanyo cylindrical cells. While the exact reason for this difference is not known, it is likely that the A&T, Panasonic, Polystor, and Sanyo prismatic cells are not fully "conditioned" for the irreversible losses of the anode. The cells were charged and discharged at different currents ranging from 20 mA to 1.0 A using an Arbin battery cycler (model BT2042, College Station, Texas). The charge/discharge measurements were also carried out at different temperatures. Cell temperatures during tests were controlled with a Tenney Jr. temperature chamber (benchtop model, Union, New Jersey). For cell impedance measurement, a Princeton Applied Research (PAR) potentiostat (model 273A) in conjunction with a 1255 Solatron Oscillator (Model 378) was used. The impedance of the Li-ion cells was measured from 65 kHz to 0.1 Hz as a function of temperature for three different

DISCLAIMER

DISCLAIMER

Portions of this document may be illegible in electronic image products. Images are produced from the best available original document.

Table 1 Physical characteristics and Capacities of Lithium-ion cell types

Manufacturer	Cell type and Dimensions (mm)	Rated cell capacity (mAh)	Measured discharge capacity (mAh) at C/20	Weight (g)	Volume (l)	Number of cells Tested
A&T	Cylindrical (17500)	800	750	25.98	0.0106	3
Panasonic	Cylindrical (17500)	780	751	24.13	0.0090	3
Polystor	Cylindrical (18650)	1250	1133	43.76	0.0168	3
Sanyo	Cylindrical (18650)	1300	1358	46.46	0.0202	2
Sanyo	Prismatic (48.3x25.4x7.6)	550	508	20.03	0.0093	2
Sony	Cylindrical (18650)	1100	1100	40.14	0.0171	5

OCVs. For current pulse measurement, a PAR potentiostat/galvanostat (model 273A) was used and the voltage response was captured with a Tektronix Oscilloscope (model THS 720).

Hybrid System Testing:

Double-layer capacitors (18mm OD by 35mm) were obtained from Panasonic (AL series Gold) rated at 2.5V and 10F capacitance. The reported resistance of each capacitor was 0.1 ohms at 1kHz. The capacitors were combined in three parallel strings of five series connected capacitors, yielding an effective capacitance of 6F and an effective resistance of 0.16 ohms.

At full charge, the cell voltage is 4.1V and the cell capacities are approximately 720 mAhr for the A&T cells and 760 mAhr for the Panasonic cells. At 25°C the Panasonic cells showed net resistance of approximately 0.15 ohms while the A&T cells were about 0.12 ohms. The resistances were quite constant at temperatures above –10°C, but increased significantly at lower temperatures, limiting the current pulse amplitudes available from these cells. The cells were stacked in series of three to yield a total stack voltage of 12.3V in the fully charged state.

The experimental plan was to first characterize the pulse performance of the cell stack at room temperature using constant current pulses of 1-5 s. The stack voltage and the individual cell voltages were monitored and the discharge program halted when the stack voltage dropped below 9V or any cell voltage dropped below 3V. These voltage limits were chosen to prevent any degradation of the CoO_2 cathode material. Cell resistances were determined from the measured voltage drop and current level during the individual pulses. The pulse repetition period was limited to about 40 s to provide a constant comparison to the other discharge profiles. After each hybrid discharge run, the cells were recharged using the Arbin test system (Arbin Model BT2042), described above which allowed accurate determination of the cell capacity prior to each run. After this initial characterization, the cells were retested in a "dumb hybrid" mode where the cells were connected in parallel to the capacitors and discharged as a single unit. Finally, the hybrid system was operated in the "smart hybrid" mode where the cells first charged the capacitors to a 9V level. The cells were then removed from the capacitors and the capacitors discharged at the constant-current rate. This sequence was repeated until the batteries exceeded the voltage- threshold criteria. A selectable series resistor that also determined the pulse repetition rate limited the current level during capacitor recharge. The system computer can be programmed to simulate any "smart" charge/discharge profile desired to determine the optimum usage of the individual cell/capacitor characteristics.

Results and Discussion

Impedance Characteristics

A typical NyQuist plot (real vs. imaginary impedance) for a fully charged (OCV = 4.1 V) Sony cell at 25°C is shown in Figure 1. It has an inductive tail in the frequency regime 65 kHz – 2.7 kHz and then a small loop followed by a larger loop. The inductive tail has

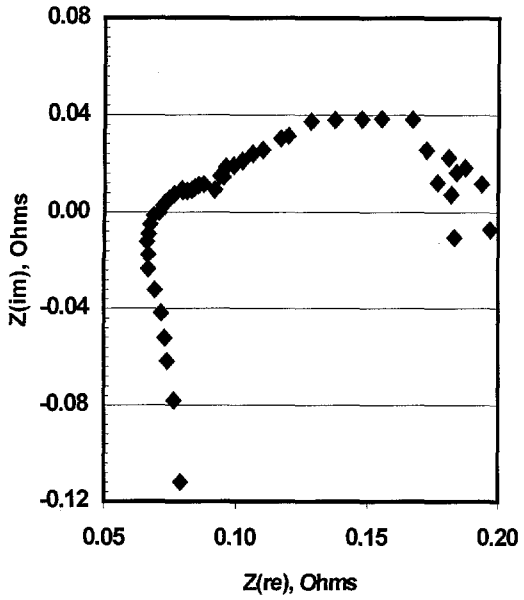

Figure 1. NyQuist plot for 18650 Sony Li-ion Cell

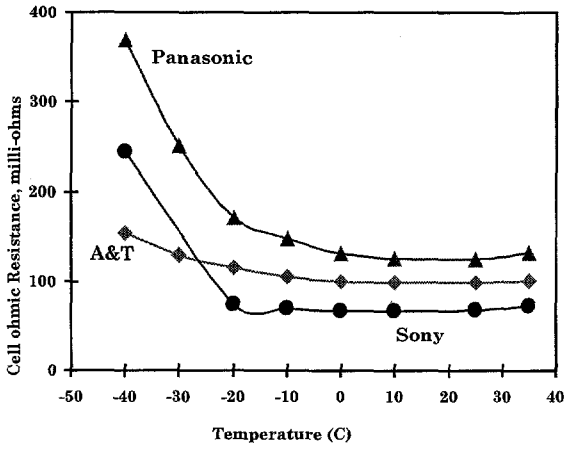

Figure 2. Cell Ohmic Resistance

been observed by others for Li-MoS_2 cells[5], and in that case has been attributed to the jellyroll and/or porous electrode designs. The inductive tail in the case of the Sony cell could also be due to a similar design feature.

The first smaller impedance loop in Figure 1 is assigned to the cathode electrolyte interface and the second loop to the anode electrolyte interface based on published data in the lithium rechargeable area[6]. The ohmic cell resistance (high frequency x-axis intercept), which includes electrolyte resistance and other resistances such as electrode bulk resistance, separator resistance, etc., in series with it, is small (~ 0.08 Ω). However, the overall cell impedance including ohmic resistance, cathode electrolyte R_{ct}, and anode electrolyte R_{ct} is higher (~ 0.18 Ω). It is clear from Figure 1 that the contribution to the cell impedance from the electrode electrolyte interface is nontrivial. The implication of this observation is that there is room to improve the power output of the cell further by optimizing the anode and cathode electrolyte

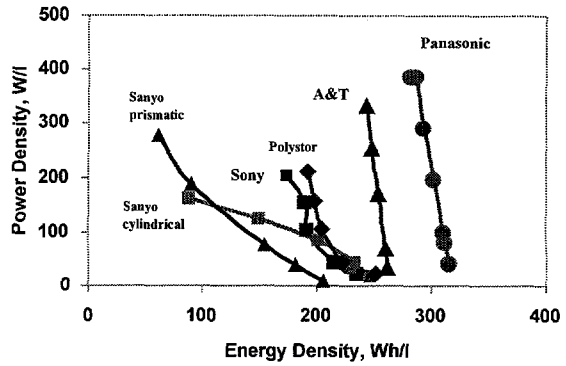

Figure 3. Energy Density vs. Power Density for Li-ion Cells

interfaces to reduce the interfacial resistance. Similar impedance behavior was observed for the other cells. In Figure 2 is shown the cell ohmic resistance at different temperatures for three Li-ion cells. The cell ohmic resistance is nearly constant between room temperature and -20°C and increases by several times at -40°C

In Figure 3 is plotted power density vs. energy density for all of the cells studied. The electrical performance of A&T and Panasonic cells is impressive. The energy and power characteristics of the tested cells from other manufacturers (Polystor, Sanyo and Sony) are inferior to those of A&T and Panasonic cells. For the Sanyo cylindrical cells, the power density reaches a plateau below 200 W/l. Between the two Sanyo Li-ion cell types, the prismatic cell exhibits higher power density than the cylindrical cell. The electrical performance of Sony cells is comparable to that of the Polystor cells. Specific energy vs. specific power data shown in Figure 3 indicates similar trends to those described above. In analyzing this data, one has to keep in mind that these cells from different manufacturers may not all represent the same generation of cells. It is entirely possible that the A&T and Panasonic cells are from a later design than the rest.

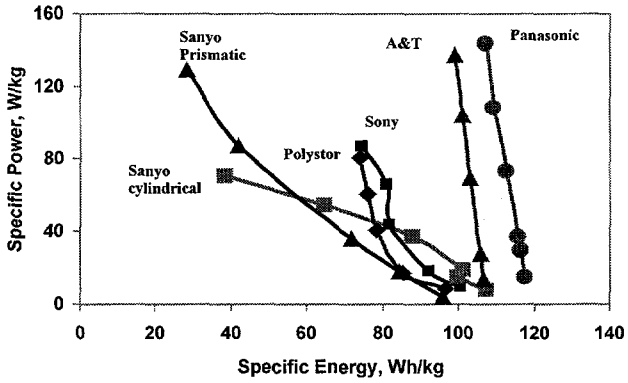

Figure 4. Specific Energy vs. Specific Power for LI-ion Cells

Operating Characteristics under Pulse Loads:

New applications such as digital wireless communications need pulse power so that more data can be packed into the available communication spectrum[7]. This demands very high current pulses for short duration from the battery pack. For example, Motorola cellular phones and NTT portable phones require current pulses of the order of 1000 mA for 0.6 ms to 7 ms. Keeping in mind this and other applications, we have evaluated the pulse performance characteristics of these cells for 1-s current

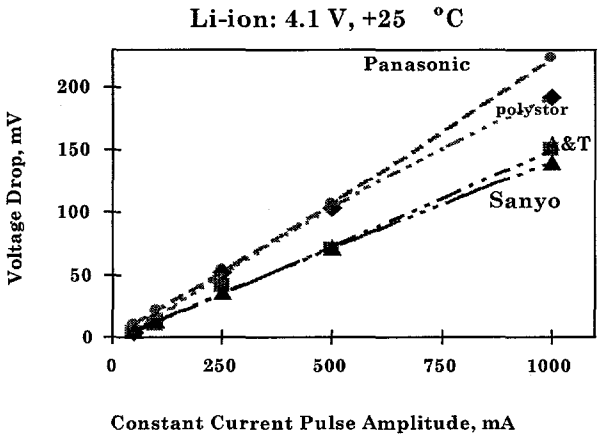

Figure 5. Voltage drop vs. Current Pulse Amplitude

pulses ranging from 50 mA to 1000 mA as a function of temperature and OCV. This technique has the advantage of measuring voltage for the complete cell under dynamic conditions.

Figure 5 shows the voltage drops at 4.1 V OCV for A&T, Panasonic, Polystor, and Sanyo cylindrical cells at 25°C. The voltage drops as a function of temperature, OCV, and current for all of the cells investigated are collected. Salient features emerging from the data are summarized below.

1) The voltage drop at 25°C (Figure 5) for the 4 cells increases linearly with increasing current, which implies that the contribution from the ohmic resistance to the voltage drop is significant.

2) At lower temperatures, especially for A&T and Panasonic cells, the voltage drop is nonlinear, which suggests that the contribution from the interfacial/ diffusional resistance is nontrivial. However, for the Sanyo and Polystor cells, which have higher capacity than A&T and Panasonic cells, the voltage drop is linear at 0°C and at –20°C, which suggests that the contribution of the interfacial/diffusional resistance is not significant in those two cases.

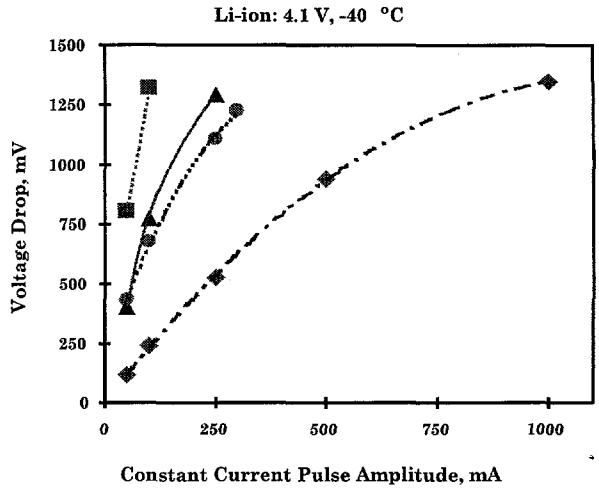

Figure 6. Voltage drop vs. Current Pulse Amplitude

3) At –40°C (Figure 6) all the cells show a nonlinear voltage drop, increasing as the temperature goes down. For example, for a 100-mA pulse, the Panasonic cell showed a 16-mV drop at 25°C, a 258-mV drop at –20°C, and a 674-mV drop at –40°C. This is typical of the other cells.

4) The voltage drop for the A&T cell is less than for the Panasonic cells for the higher temperatures studied, but at –40°C the A&T cell voltage drop is higher than the Panasonic cell.

5) A&T, Panasonic and Sanyo cells cannot be pulsed at very high currents at –40°C.

6) The voltage drop for current and temperature in general increases slightly with depth of discharge (more depth of discharge lowers OCV). For example, at –20°C and 100-mA pulse the Panasonic cells showed a voltage drop of 258 mV at 4.1 V OCV (fully charged); 280 mV at 3.6 V OCV (partially discharged); and 287 mV at 3.1 V OCV (nearly completely discharged).

7) The cell resistance computed from the voltage drop is comparable to the total cell resistance obtained from the impedance measurement, especially near ambient temperature.

Hybrid Test Results

Pulse Performance at 25 °C

Direct discharge of the cells at constant-current pulses of 1-5 s resulted in almost full cell capacities being realized up to current levels of about 3A for the Panasonic cells and about 4A for the A&T cells. Above this level, the usable cell capacities quickly dropped. The measured cell capacities for all discharge modes are shown in Figures 7 and 8 for the Panasonic and A&T cells, respectively.

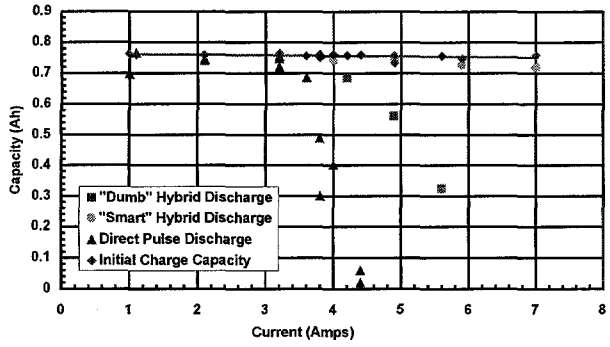

Figure 7. Load capacity of Panasonic Cells under direct and hybrid pulse conditions.

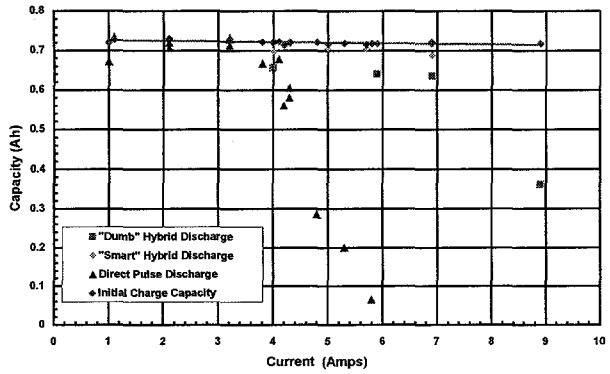

Figure 8. Load capacity of A&T Cells under direct and hybrid pulse conditions.

The open circuit voltage and the cell resistance determine the usable cell capacity at a given current for a fixed voltage threshold. Figure 9 shows the voltage profiles for the stack and individual cells during discharge. The voltage drop during pulsing was used to calculate the resistance as shown in Figure 10. The cell resistances remained fairly constant over the cell discharge range until the very end of cell life when the cell resistance began to increase.

Pulsing the cells in the "dumb hybrid" mode resulted in extended cell capacity usage for both cell types. Figures 7 and 8 show that the Panasonic cells supported about a 50% increase in pulse current level (3.8A to 5.6A) while the A&T cells obtained about a 100% increase (4.8A to 8.9A). The effective resistance of this cell/capacitor hybrid changes as a function of time, initially showing capacitor-like characteristics and then behaving like the cell at longer times. The resistance can be expressed as:

$$R_{eff} = \frac{R_{batt}\,(R_{cap} + t/C)}{R_{batt} + R_{cap} + t/C}$$

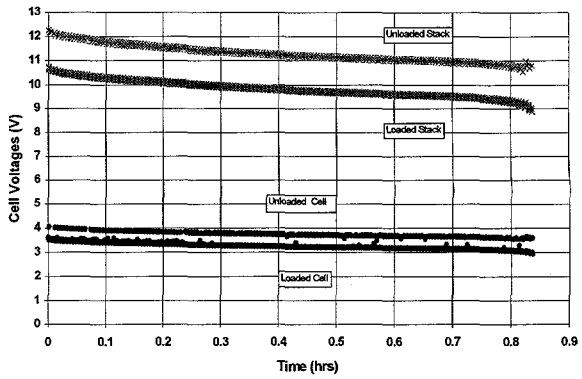

Figure 9. Direct discharge voltage profiles for pulsed A&T cells.

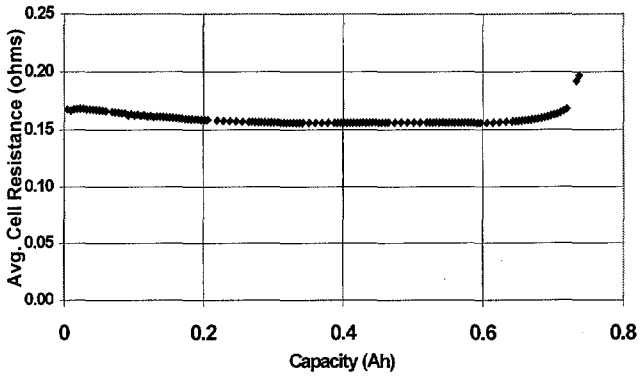

Figure 10. Measured cell resistance during direct pulsing of A&T cells.

At $t = 0$: $R_{eff} = \frac{R_{batt} R_{cap}}{R_{batt} + R_{cap}}$

And at long times: $R_{eff} = R_{batt}$

For the A&T cells, the calculated effective single cell resistances at t=0 are:

R_{batt}= 0.16 ohm R_{cap}= 0.056 ohm R_{eff} = 0.04 ohm.

Operation of the system in the "smart hybrid" mode allows the cells to used in their most efficient, low current mode for capacitor charging while using the capacitors for the high-power pulses. Again looking at Figures 7 and 8 at the "smart hybrid" data, cell capacities over 98% of original charge values were obtained. A selectable series resistor limited the cell currents during the charging period. Peak charging currents of up to 750 mA with an average charging current of 500 mA were

typical during these runs. The high measured cell capacities indicate that the resistor did not result in any significant energy loss. Lower charging currents would result in even more efficiency, especially at lower temperatures.

Pulse Performance at -20 °C

At temperatures below -10°C, cell resistance increases rapidly, significantly limiting the available cell capacity. More of the electrochemical capacity of the cell can be accessed if the cells are used in a low-current charging mode as employed by the "smart hybrid" system. As a test of this system under these conditions, the Panasonic cells were cooled to -20°C and connected to the hybrid test system. The capacitors remained at room temperature for these measurements. The cells were initially discharged by direct current pulses and then used in the capacitor recharge mode. Table I below lists the discharge conditions and shows that a factor of five improvement in capacity was obtained. Lower charging currents would result in even more efficient use of the cell capacities.

Table I.

	Pulse(A)	Pulse(s)	Avg.Cell(A)	Capacity(Ahr)
Direct	0.53	4		0.024
Hybrid	4	4	0.34	0.129

Conclusions

A number of Li-ion cells from different manufacturers were evaluated for their electrical and electrochemical characteristics as a function of temperature and OCV. Electrolyte resistance remained nearly constant from 35°C to –20°C in all cases and then increased by 2 to 3 times at –40°C. The electrolyte resistance of the cells was only a few hundred milliohms, which is similar to that of Ni/Cd and Ni/MH cells of comparable size. Electrolyte resistance was also nearly independent of state-of-charge (OCV).

In the temperature range 35°C to –20°C, where the electrolyte resistance remains almost constant, the voltage drop for a given current pulse increased with decreasing temperature. Although the electrolyte resistance alone cannot explain this trend, the total cell impedance (including electrolyte resistance, interfacial charge transfer resistances, and Warburg impedance) did increase with a decrease in temperature. The voltage drop for a given current and temperature roughly corresponds to the total cell impedance. Further, our impedance data indicate that the contribution from the interfacial charge transfer resistance and diffusional impedance to the total cell impedance is quite significant at lower temperatures and the interfacial resistance of the anode is higher than that of the cathode. One has to keep this high R_{ct} in mind when optimizing the cell design for both high energy and power. Generally, the cell resistance computed from the voltage drop is comparable to the total cell resistance obtained from the a-c impedance measurement, especially near ambient temperature. However, at lower temperatures, the voltage drop measurement yields a lower resistance, which might be due to an increase of the internal temperature of the cell caused by pulsing.

We have also evaluated the charge/discharge characteristics of the cells at different temperatures and at different charge/discharge currents. The Ragone data obtained from measuring the discharge capacity at different discharge currents indicates that the Li-ion cells possess a favorable combination of energy and power. The energy and power densities at room temperature could be as high as 320 Wh/l and 380 W/l, respectively. Evaluation of charge/discharge characteristics of the Li-ion cells at subambient temperatures is planned.

A hybrid cell/capacitor tester was used to demonstrate extended performance of Li-ion batteries under pulsed-current conditions. Parallel coupling of the cells and capacitors resulted in a reduction of system resistance, allowing extended discharge periods for cells with fixed discharge voltage criteria.

References

1) G. Nagasubramanian and Rudy Jungst, *J. Power Sources* **72,** 189(1998).

2) G. Nagasubramanian, P. Roth, R. Jungst, and N. Clark , *The 15th International Seminar & Exhibit on Primary & Secondary Batteries* March 2-5, 1998 Fortlauderdale, Fl.

3) P. J. Cygan, T. B. Atwater, and L. P. Jarvis, *The 13th Annual Battery Conference on Applications and Advances,* Long Beach California January 13-16, 1998.

4) M. J. Isaacson, B. J. Kraemer, T. J. Laramore, S. T. Mayer, and L. C. Josephs, *Proceedings of the 37th Power Sources Conference,* Cherry Hill, NJ, June 17-20, 1996.

5) F. C. Laman, M. W. Matsen, and J. A. R. Stiles, *J. Electrochemical Soc.* **133,** 2441(1986).

6) K. Ozawa *Solid State Ionics* 69, 212(1994).

7) A. Anani, F. Eschbach, J. Howard, F. Malaspina, and V. Meadows, *Electrochimica Acta*, 40 2211(1995).

Acknowledgement

Sandia National Laboratories is a multiprogram laboratory operated by Sandia Corporation, a Lockheed Martin Company, for the United States Department of Energy under contract DE-AC04-94AL85000.